Timelike Compton Scattering

1. Introduction

The EpIC generator was used to simulate Timelike-Compton Scattering (TCS), the Bethe-Heitler (BH) process (which interferes with it at the amplitude level) and the TCS-BH interference, all together. Both TCS and BH processes involve the following particles in the initial and final states: $\gamma + p \to p' + \gamma^* \to p' + e^+ + e^-$. At EIC, the initial photon is a quasi-real photon exchanged in electron scattering at very low Q^2.

The generated events, one million with each electron helicity for the highest and lowest nominal collider energy settings (5×41 GeV and 18×275 GeV) were passed through the full ATHENA GEANT4 simulation. This document provides additional information on the simulation study, to complement the ATHENA detector proposal. All distributions shown have been scaled to represent the yield at 10 fb^{-1}.

Assuming reconstruction of the scattered electron via missing mass and missing momentum (see Sec. 2.3), 85% of the generated events at the lowest collision energy (5×41 GeV) were reconstructed with a proton and the two produced leptons. At the highest collision energy (18×275 GeV), this fraction falls to 30% (due to the far-forward proton detection acceptance at the lowest $|t|$ for these kinematics). However, the cross-section itself is approximately 2.5 - 3 times higher at these kinematics, which compensates the loss in statistics.

2. Event kinematics

2.1. Q^2

The Q^2 is the virtuality of the initial-state photon which scatters from the nucleon, defined as $Q^2 = -(k - k')^2$, where k and k' are the four-momenta of the beam and scattered electron, respectively.

The generated Q^2 distribution, the shape of which is independent of electron energy, can be seen in Fig. 1. Events were generated up to $Q^2 = 0.15$ GeV^2, covering the photoproduction part of the phase-space.

2.2. Q'

The Q' is the invariant mass of the produced virtual photon in the scattering: $Q'^2 = (l^+ + l^-)^2$, where l^+ and l^- are the four-momenta of its decay-leptons.

The Q' was generated in the range $2 < Q'^2 < 20$ GeV^2, where the lowest edge was motivated by the fact that Q' provides the hard scale in the TCS process and so needs to be sufficiently high, while the upper edge was motivated by the decrease of the cross-section with increasing Q'. The distribution is reconstructed with uniform efficiency across the full generated range (Fig. 2). The region around the mass of the J/Ψ will be cut out in analysis, to avoid contamination of the TCS-BH signal with

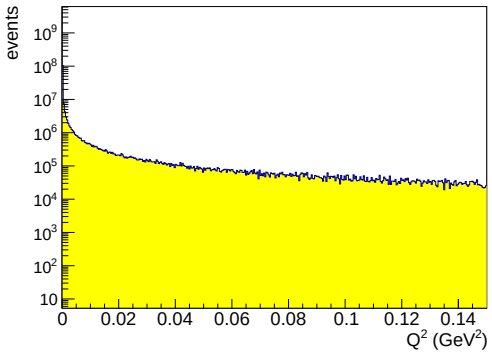

Figure 1. Generated Q^2 distribution, showing the TCS-BH yield for integrated luminosity of 10 fb^{-1} at 18×275 GeV collision energy.

photoproduction of charmonium.

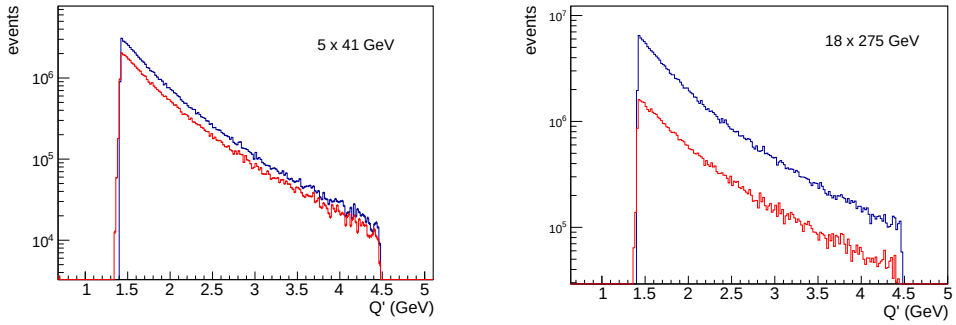

(a) 5×41 GeV (b) 18×275 GeV

Figure 2. Generated (blue) and reconstructed (red) Q' for the low and high collision energies. Integrated luminosity of 10 fb^{-1}.

2.3. $\sqrt{s}$

The $\sqrt{s}$ is the CoM mass of the photon-proton system, defined as $s = (q + p)^2$, where q and p are the four-momenta of the initial-state quasi-real photon and of the beam proton, respectively.

The $\sqrt{s}$ of the event is highly dependent on the collision energy – generated and reconstructed distributions can be seen in Fig. 3.

2.4. τ

The kinematic variable $\tau = \frac{Q'^2}{2\mathbf{p}\cdot\mathbf{q}} = \frac{Q'^2}{s - m_p^2}$, where m_p is the nucleon mass, plays a similar role to x_B in Deeply Virtual Compton Scattering. It is related to the longitudinal momentum fraction, x, carried by the struck quark. The generated and reconstructed distributions at low and high collision energies can be seen in Fig. 4.

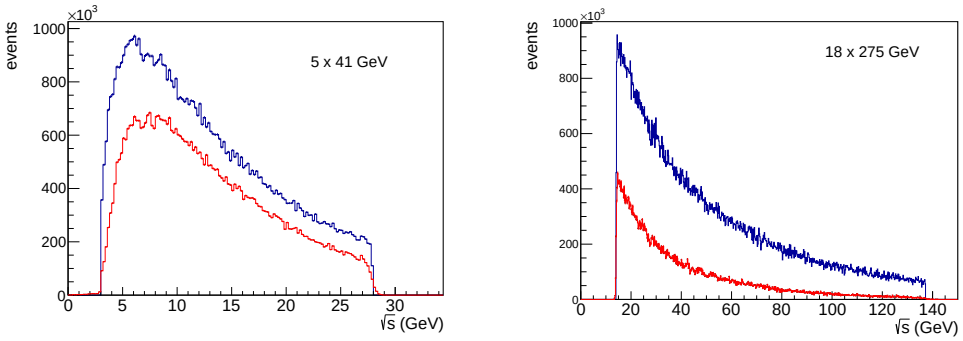

(a) 5×41 GeV (b) 18×275 GeV

Figure 3. Generated (blue) and reconstructed (red) $\sqrt{s}$ for the low and high collision energies. Integrated luminosity of 10 fb^{-1}.

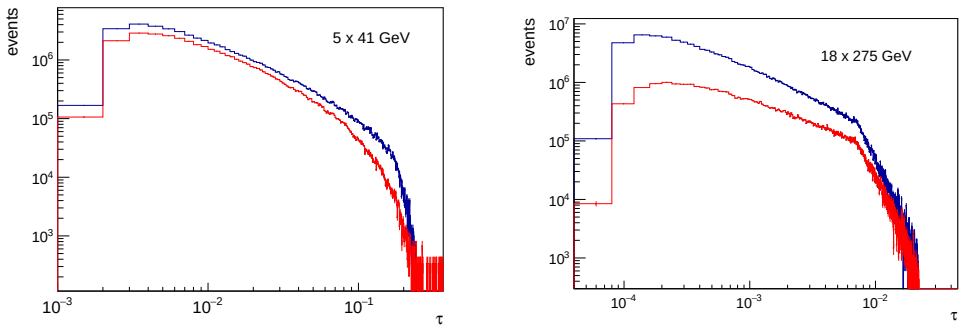

(a) 5×41 GeV (b) 18×275 GeV

Figure 4. Generated (blue) and reconstructed (red) τ for the low and high collision energies. Integrated luminosity of 10 fb^{-1}.

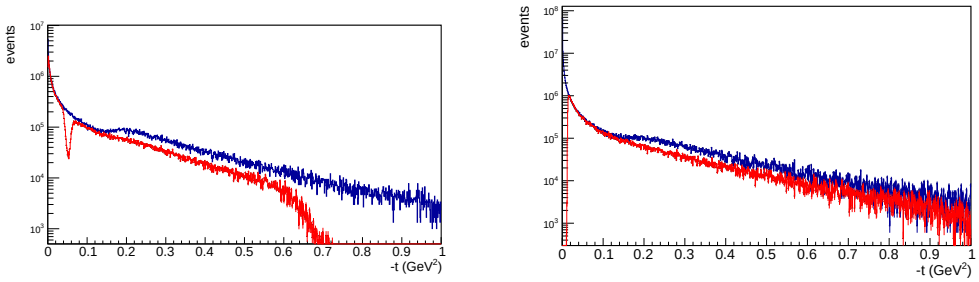

(a) 5×41 GeV (b) 18×275 GeV

Figure 5. Comparison between the generated (blue) and reconstructed (red) $|t|$ distributions for lowest and highest collision energies. Integrated luminosity of 10 fb^{-1}.

2.5. t

The Mandelstam variable $t = (p' - p)^2$, where p and p' are the four-momenta of the beam and recoil proton, respectively, quantifies the four-momentum transfer to the proton as a result of the scattering. The Generalised Parton Distribution (GPD) formalism used to describe the TCS process is defined at low t. The Fourier-transform of a GPD with respect to t reveals the distribution in impact parameter space. It is therefore important to measure across a sufficiently wide range in t, from the lowest values accessible. The generated and reconstructed distributions at the lowest and highest collision energies are shown in Fig. 5. A dip in the reconstructed t-distribution at the low collision energies corresponds to the transition between the Roman Pots (which are used to measure events at the lowest t) and the B0 spectrometer (which provides the acceptance for larger values of t). The position of the dip can be moved by changing the beam energies, thus covering the full phase-space.

2.6. θ

The variable θ is the angle between the momenta of the produced positive lepton l^+ and the recoiling proton, calculated in the CoM frame of the produced lepton-pair.

The θ distribution, which was generated in the region $\pi/6 < \theta < 5\pi/6$ radians to avoid the edges at which the BH contribution grows dramatically, is shown in Fig. 6. The full range of θ is reconstructed, showing consistent efficiency at the highest collision energy and a small θ-dependence in the efficiency for the lowest collision energy.

2.7. ϕ

The Trento ϕ is the angle between the hadronic plane (defined by the (quasi-)real photon and recoil proton), and the leptonic plane (defined by the produced leptons). The photon polarisation induces an asymmetry in the TCS process, which depends on the Trento ϕ. The integrated ϕ distributions for the generated and reconstructed events can be seen in Fig. 7.

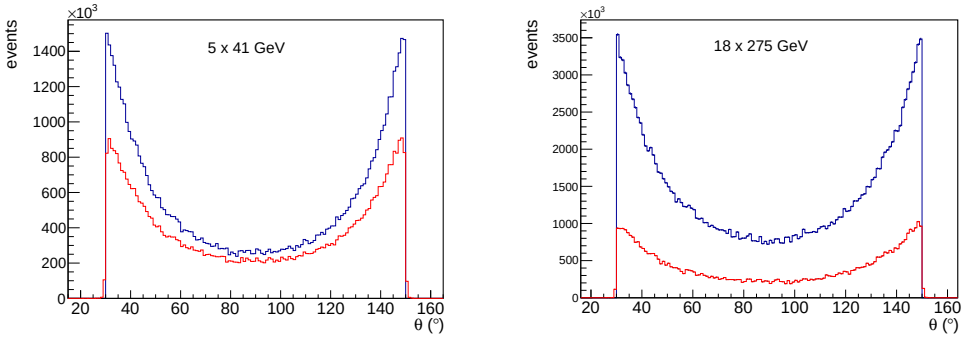

(a) 5×41 GeV (b) 18×275 GeV

Figure 6. Generated (blue) and reconstructed (red) θ for the low and high collision energies. Integrated luminosity of 10 fb^{-1}.

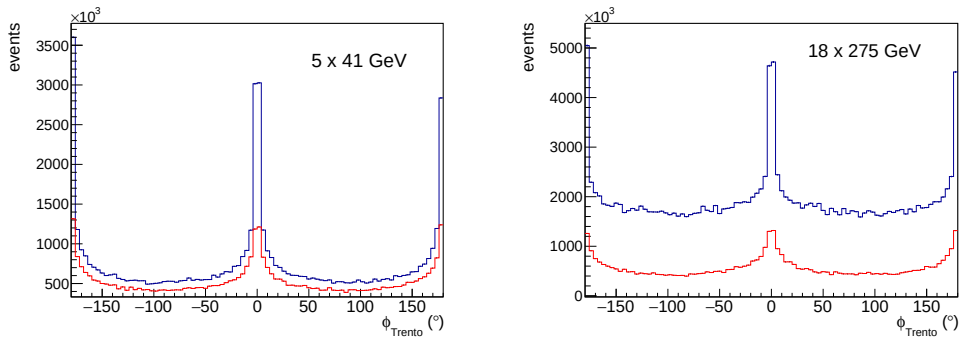

(a) 5×41 GeV (b) 18×275 GeV

Figure 7. Generated (blue) and reconstructed (red) Trento ϕ for the low and high collision energies. Integrated luminosity of 10 fb^{-1}.

3. Particle momentum and pseudo-rapidity

3.1. Produced leptons

The e^+e^- pair are produced at mid-rapidity for all collision energies and are detected in the central detector with almost perfect efficiency (92% - 94% from the lowest to the highest collision energies): Figs. 8 - 9. The produced virtual photon in TCS and BH has a roughly equal probability of decaying into a $\mu^+\mu^-$ pair – these pairs have the same distribution as e^+e^-. Detection of muons in these kinematics can therefore increase the measured statistics of the TCS-BH channel by up to a factor of 2.

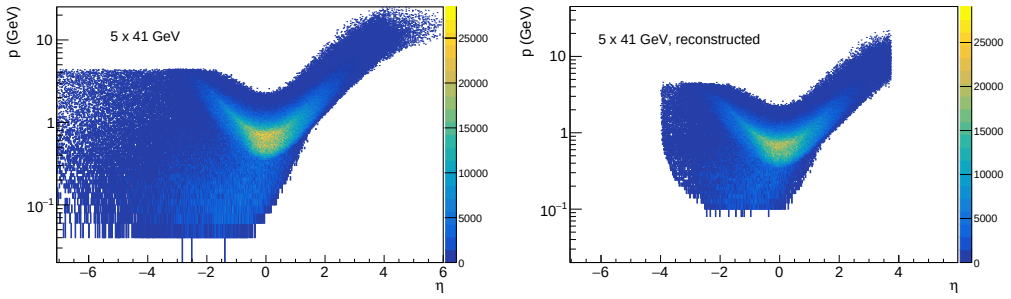

(a) Generated (b) Reconstructed (full simulation)

Figure 8. Momentum vs. pseudo-rapidity of the produced e^+e^- for the 5×41 GeV collision energy. Integrated luminosity of 10 fb^{-1}.

3.2. Recoil proton

The TCS process takes place at low t, where the proton recoils at very low angles, extremely close to the beam-line. At the highest collision energies, the recoil proton is detected entirely in the Roman Pots (Fig. 10, which also shows the effect of the crossing angle: the recoil protons are clumped around a pseudo-rapidity corresponding to 25 mrad). At low collision energies, however, the recoil proton is detected in the Roman Pots for events with the lowest t and in the B0 spectrometer for higher t (Fig. 11). A dip in the reconstructed t-distribution corresponds to the transition between these two detectors and is unavoidable (Fig. 5). The position of the dip depends on the collision

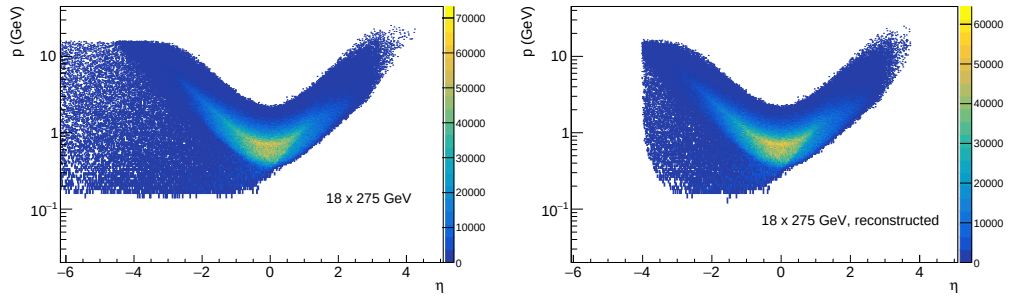

(a) Generated (b) Reconstructed (full simulation)

Figure 9. Momentum vs. pseudo-rapidity of the produced e^+e^- for the 18×275 GeV collision energy. Integrated luminosity of 10 fb^{-1}.

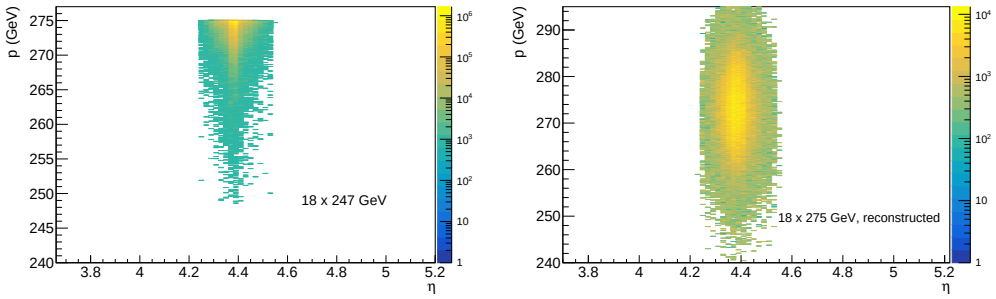

(a) Generated (b) Reconstructed

Figure 10. Momentum vs. pseudo-rapidity of recoil protons for the 18×275 GeV collision energy, in the lab frame where the $-z$ axis is defined as the electron beam direction. Integrated luminosity of 10 fb^{-1}.

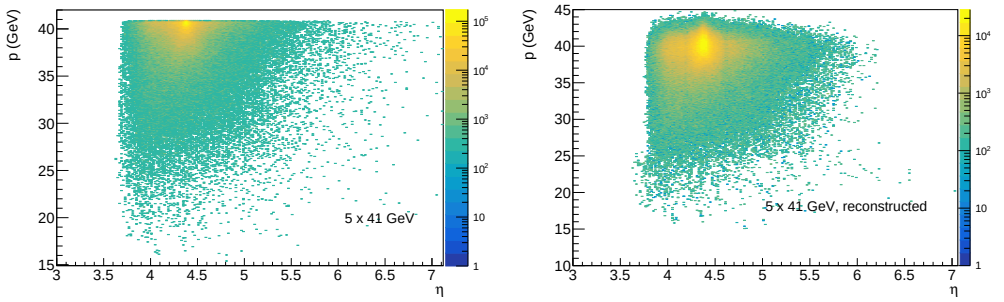

(a) Generated (b) Reconstructed

Figure 11. Momentum vs. pseudo-rapidity of recoil proton for the 5×41 GeV collision energy, in the lab frame where the $-z$ axis is defined as the electron beam direction. Integrated luminosity of 10 fb^{-1}.

energy – thus full acceptance in t can be obtained by varying the beam energies.

3.3. Scattered electron

The TCS process involves the scattering of a real (or quasi-real) photon from a nucleon or nucleus. The extremely low Q^2 requirement of the photon in the initial state (simulated for $Q^2 < 0.15$ GeV^2) means the beam electron is scattered at extremely low angles, in the very far-backward direction (Fig 12). At the lowest collision energy (5×41 GeV), approximately 10% of the scattered electrons (those with the lowest $|\eta|$) will be detected by the electron endcap in the central barrel. At the highest collision energy, practically all the electrons scatter outside of the central detector acceptance. The low-Q^2 tagger will therefore be highly instrumental in detecting part of the high $|\eta|$ scattered electron distribution at all collision energies and enabling fully exclusive reconstruction. The rest of the scattered electrons will go undetected – exclusivity of the process will be ensured through cuts on missing momentum and missing mass.

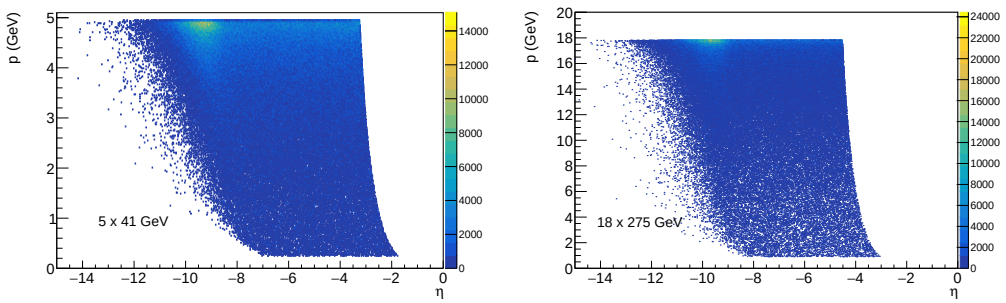

(a) 5×41 GeV (b) 18×275 GeV

Figure 12. Generated momentum vs. pseudo-rapidity of scattered electron. Integrated luminosity of 10 fb^{-1}.